ELSEVIER

Agricultural and Forest Meteorology 105 (2000) 195–214

AGRICULTURAL AND FOREST METEOROLOGY

www.elsevier.com/locate/agrformet

Analysis of the limits of the $C_T{}^2$-profile method for sensible heat flux measurements in unstable conditions

J.-P. Lagouarde [a,*], A. Chehbouni [b,1], J.-M. Bonnefond [a], J.-C. Rodriguez [b], Y.H. Kerr [c], C. Watts [b], M. Irvine [a]

[a] *Unité INRA de Bioclimatologie, Domaine de la Grande Ferrade, BP 81, 33883 Villenave d'Ornon, France*
[b] *IRD/IMADES, Hermosillo CP 83190, Sonora, Mexico*
[c] *CESBIO (CNES-CNRS-UPS), 18 Avenue E. Belin, 31401 Toulouse Cedex 4, France*

Abstract

We present a test of the $C_T{}^2$-profile method described by Hill et al. [J. Atmos. Ocean. Technol. 9 (5) (1992) 526] to estimate the surface sensible heat flux over an homogeneous surface. A comparison with traditional eddy correlation measurements performed over a pasture (during the SALSA-Mexico experiment) using three identical large aperture scintillometers (LASs) along a 330 m propagation path and placed at heights 2.50, 3.45 and 6.45 m is first given. Scintillometer derived fluxes using the classical method at one level [Agric. For. Meteorol. 76 (1995) 149] reveal that the three scintillometers provide consistent measurements but underestimate by 15% the flux obtained with the 3D sonic anemometer. This is attributed to spatial non-homogeneities of the experimental site. Considerable scatter (and even the impossibility of performing computations) is found when using the $C_T{}^2$-profile method which is particularly prone to errors in nearly neutral and highly unstable conditions. The sensitivity of these errors to the accuracy of scintillometer measurements, the calibration errors and the measurement heights is investigated numerically. Simulations are made assuming a normal distribution of the relative error for $C_N{}^2$ with standard deviations σ between 2 and 5% and no calibration error in a first step. Only calibration errors (up to 4% between instruments) are simulated in a second step. They confirm that the profile method degrades very rapidly with the accuracy of $C_N{}^2$: for instance the RMS error for H reaches 68 W m^{-2} (and the cases of impossible computation 28%) for a realistic $\sigma = 5\%$ value, with heights 2.50 and 3.45 m. Results appear slightly less sensitive to small calibration errors. The choice of the measurement heights z_1 and z_2 is also analysed: a ratio $z_2/z_1 \sim 3$ or 4 with $z_1 > 2$ m seems the best compromise to minimise errors in H. Nevertheless the accuracy of the profile method is always much lower than that given by the classical method using measurements at one level, provided a good estimate of roughness length is available. We conclude that the $C_T{}^2$-profile method is not suitable for routine applications.

Keywords: Atmospheric turbulence; Sensible heat flux; Optical scintillation; Structure parameter; Large aperture scintillometer

1. Introduction

Recent modelling efforts concentrate on improving the parameterisation of land-surface processes in atmospheric models or environmental modelling (Noilhan and Lacarrère, 1995; Brunet, 1996). Up-scaling is now an important topic and several approaches, such as aggregation techniques have been developed to account for the effect of surface heterogeneity in models (Avissar, 1991; Raupach, 1995; Raupach and Finnigan, 1995; Chehbouni et al., 1995). However, the validation of simulations at regional

* Corresponding author.
E-mail address: lagouarde@bordeaux.inra.fr (J.-P. Lagouarde).
[1] Present address: IRD, 213 rue La Fayette, 75480 Paris, France.

0168-1923/00/$ – see front matter
PII: S0168-1923(00)00192-1

(and obviously larger) scales still remains a critical issue.

Due to their ability to integrate atmospheric processes along a path length which dimension may range between a few hundred metres to a few kilometres, optical methods based on the analysis of scintillations appear as an interesting alternative to classical micrometeorological methods, such as eddy correlation, which can only provide local fluxes, typically at the scale of the order of 100 m. A review of scintillation techniques can be found in Hill (1992). In what follows, we will focus on the use of large aperture scintillometers (LASs). It has been shown by various authors (e.g. Hartogensis, 1997) that LAS could deliver areally averaged sensible heat fluxes over path lengths of up to several kilometres. Since the LAS provides indirect estimate of the temperature scale T_*, a major practical difficulty in using a single LAS instrument for deriving the path-averaged sensible heat flux is related to the fact that an independent estimate of friction velocity (u_*) is required. The latter is often determined from a measurement of wind speed combined with an estimation of roughness length. Above a complex surface, this requires assuming that the Monin–Obhukov similarity is conserved and also that an aggregation scheme for roughness is known. An optical means of inferring friction velocity u_* for practical applications is tempting, even though it does not eliminate the need for Monin–Obukhov similarity theory (MOST) to be valid.

In this regard, Green et al. (1997) tested the 'Inner Scale Meter' (ISM) which employs both large aperture and laser scintillometers. This method is based on the dependence of laser measurements upon u_*. But laser scintillometers are practically limited to distances less than a few hundred meters (typically comprised in the range ~100–250 m according to literature results) depending on the strength of the refractive turbulence and of the height. This makes the ISM not suitable for larger scales. Andreas (1988) used two LAS over the same path length to infer the average Monin–Obukhov length. Hill et al. (1992) tested this method, referred to as the '$C_T{}^2$-profile method' and described below, using two LAS at different heights (1.45 and 3.95 m) over a 600 m propagation path to estimate heat and momentum surface fluxes. But their experiment suffered from systematic differences between $C_N{}^2$ values measured by the two scintillometers and their data set was limited to a few runs. They showed the reliability of retrieved sensible heat fluxes was significantly affected by the accuracy of the instruments used. Nieveen and Green (1999) recently described a new test of the method over a pasture land; however, a questionable experimental set-up with the two scintillometers sampling very different propagation paths (3.1 km at 10 m, and only 141 m at 1.5 m), and inhomogeneous surface conditions limit the validity of this test. To the authors' knowledge, no other tests of the $C_T{}^2$-profile method have been published.

Before using such an approach over composite terrain, it is therefore necessary to test the method further over a homogeneous surface. This paper presents experimental results obtained during summer 1998 over a pasture in Mexico within the framework of the SALSA (semi-arid-land-surface-atmosphere) program (Goodrich et al., 1998). Numerical simulations are then performed to investigate the effect of different sources of errors, and to evaluate the impact of the measurement heights on the flux retrieval accuracy.

2. Theory

2.1. General definitions

Scintillometers provide a measurement of the refractive index structure parameter $C_N{}^2$ in the atmosphere. In the optical domain, $C_N{}^2$ mainly depends on temperature fluctuations in the atmosphere and only slightly on humidity fluctuations. The temperature structure parameter $C_T{}^2$ can be derived from the refractive index structure parameter $C_N{}^2$ by

$$C_T{}^2 = C_N{}^2 \left(\frac{T_a{}^2}{\gamma P}\right)^2 \left(1 + \frac{0.03}{\beta}\right)^{-2} \quad (1)$$

The corrective term including the Bowen ratio β takes into account the influence of humidity fluctuations.[2] P is the atmospheric pressure (Pa), T_a the air temperature (K), and γ the refractive index for air ($\gamma = 7.9 \times 10^{-7}$ K Pa^{-1}). $C_N{}^2$ and $C_T{}^2$ are in m$^{-2/3}$ and K^2 m$^{-2/3}$, respectively. $C_T{}^2$ and the temperature scale T_* (K) are related by

[2] It is worth noting that in recent papers (Green et al., 1994; McAneney et al., 1995; Lagouarde et al., 1996) Eq. (1) is given incorrectly. The term $(1 + 0.03/\beta)$ should be to the power -2 as indicated here.

$$C_T{}^2 = T_*{}^2 z^{-2/3} f\left(\frac{z}{L}\right) \quad (2)$$

where z is the height corrected from the displacement height d. T_* is classically defined as $w'\theta'/u_*$ ($w'\theta'$ being the kinematic heat flux, cross product of the vertical wind speed and temperature fluctuations). The expressions of the function f vary according to authors (Kaimal and Finnigan, 1994; De Bruin et al., 1995). Following Hill et al. (1992), we use those proposed by Wyngaard (1973)

$$f\left(\frac{z}{L}\right) = 4.9\left(1 + 7\left|\frac{z}{L}\right|\right)^{-2/3} \quad \text{for unstable conditions, } \frac{z}{L} \le 0 \quad (3)$$

$$f\left(\frac{z}{L}\right) = 4.9\left(1 + 2.4\left|\frac{z}{L}\right|^{2/3}\right) \quad \text{for stable conditions, } \frac{z}{L} > 0 \quad (4)$$

L is the Monin–Obhukov length defined as

$$L = \frac{T_a u_*{}^2}{kgT_*} \text{ with } k = 0.4 \text{ and } g = 9.81\,\mathrm{m\,s^{-2}} \quad (5)$$

2.2. Estimation of the sensible heat flux from measurements at one level

As this method (referred to as '1L method' in what follows) has been described in detail by several authors (McAneney et al., 1995; De Bruin et al., 1995), we shall only briefly recall its principle. T_* is retrieved from the scintillometer measurements according to (1) and (2). A wind speed measurement allow the determination of u_* from the wind profile equation, which requires the roughness length z_0 to be known

$$u_* = ku\left[\ln\left(\frac{z}{z_0}\right) - \Psi_M\left(\frac{z}{L}\right)\right]^{-1} \quad (6)$$

where Ψ_M is the classical stability function given by Panofsky and Dutton (1984).

The sensible heat flux H ($\mathrm{W\,m^{-2}}$) is then computed as

$$H = \rho c_p u_* T_* \quad (7)$$

ρ ($\mathrm{kg\,m^{-3}}$) and c_p ($\mathrm{J\,kg^{-1}\,K^{-1}}$) are the air density and heat capacity, respectively. u_* is in $\mathrm{m\,s^{-1}}$. Since the sensible heat flux determines atmospheric stability, which in turn influences turbulent transport, an iterative procedure is necessary to compute z/L, Ψ_M and thence u_*. An initial computation is made assuming neutrality ($z/L = 0$). The value of H obtained allows a better estimation of T_* and u_* through Eqs. (1)–(6), which provides a new approximation of H. The procedure is repeated until the convergence on z/L is obtained.

2.3. Estimation of the sensible heat flux using $C_T{}^2$-profile method

In what follows, low and high levels will be referenced by indices 1 and 2, respectively. The ratio of the $C_T{}^2$ measurements at both levels leads through Eq. (2) to

$$r = \frac{f(z_1/L)}{f(z_2/L)} \quad (8)$$

with

$$r = \frac{C_{T_1}{}^2}{C_{T_2}{}^2}\left(\frac{z_1}{z_2}\right)^{2/3} \quad (9)$$

Eqs. (8) and (9) assume that fluxes (and hence T_*) are constant with height. In other words it assumes that MOST applies, which requires a laterally homogeneous surface layer. L can be estimated by solving Eq. (8). Eqs. (3) and (4) show that the function f decreases with z for unstable conditions while it increases in the case of stability. A test on r therefore allows to discriminate between stable and unstable conditions ($r < 1$ or $r > 1$, respectively). For unstable conditions, Eqs. (3) and (8) lead to

$$L = 7\frac{z_1 r^{3/2} - z_2}{r^{3/2} - 1} \quad (10)$$

The constraint $L < 0$ imposes a second condition on r, which leads to $1 < r < (z_2/z_1)^{2/3}$. It can easily be seen that this second condition can also be found as the limit of r defined by Eqs. (3) and (8) when $z/L \to -\infty$. Similarly, in the stable case, Eqs. (4) and (8) give

$$L = \left[2.4\frac{r z_2{}^{2/3} - z_1{}^{2/3}}{1 - r}\right]^{3/2} \quad \text{with } \left(\frac{z_1}{z_2}\right)^{2/3} < r < 1 \quad (11)$$

Eq. (2) applied to any level which then allows to compute T_* while u_* is derived from Eq. (5). H is finally given as before by Eq. (7).

3. Experiment

3.1. Site and experimental set-up

The experiment was performed during August and September 1998 and was part of the SALSA program (Goodrich et al., 1998). The site is situated in the vicinity of the Zapata village in the upper San Pedro basin (31°01′N, 110°09′W), north of Mexico (Sonora). The altitude is 1450 m ASL. The site is a large plain displaying some large but gentle undulations (several hundreds of metres wide with elevations reaching about 15 m).

The experimental set-up was placed in the middle of a very flat area (Fig. 1a) so as to have the best fetch conditions as possible. A gentle slope was situated about 300 m to the south. A line of sparse small trees was located about 400 m north along a temporary drainage stream. In the other directions the fetch was even better.

The vegetation is a natural grassland used for extensive cattle breeding. It is composed mainly of perennial grasses, with dominant species being black grama (*Bouteloua eriopoda*) and hairy grama (*Bouteloua hirsuta*). The height of grass varied between 20 and 60 cm during the period of the experiment. Some local heterogeneity within the field developed after rainfalls. Particularly a wide homogeneous area of denser and higher green vegetation totally covering the ground appeared in the western part of the field (which was even flooded during a few hours after a storm). Elsewhere the vegetation was lower and somewhat drier, with a mean cover estimated to be around 70%; it was quite representative of the rest of the site, with local non-homogeneities lower than a few metres.

Three identical LASs built by the Meteorology and Air Quality Group (Wageningen Agricultural University, the Netherlands) were installed in parallel along a 330 m path oriented NE–SW (43° from north), which is perpendicular to the prevailing winds. These instruments were built according to the method described in Ochs and Cartwright (1980) and Ochs and Wilson

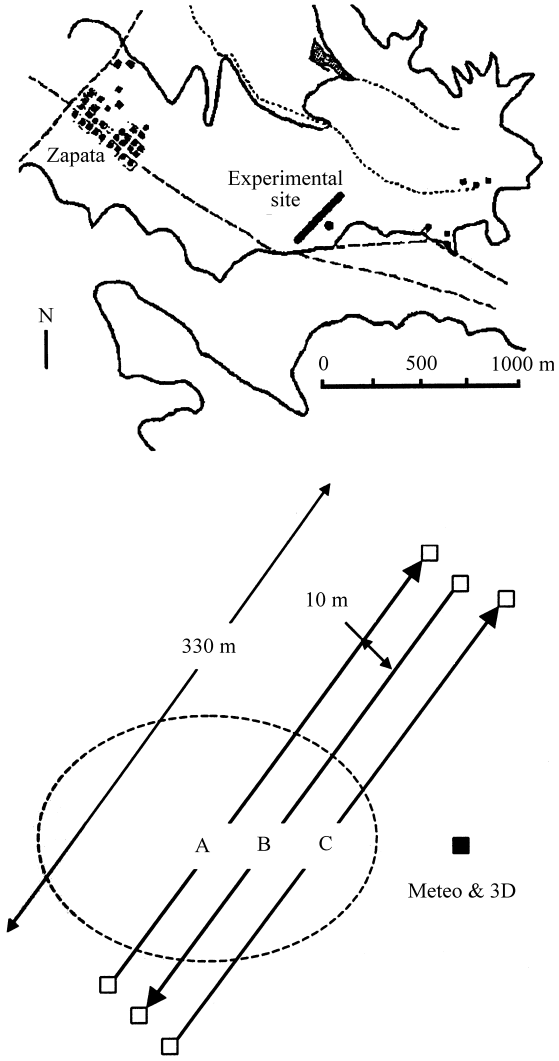

Fig. 1. (a) Zapata experimental site; the propagation path of the scintillometers is indicated by a thick segment, and the location of the meteorological and 3D reference measurements by a dot. (b): Location of the scintillometers (A, B, C); the square dot corresponds to the location of the 3D sonic anemometer and of the micrometeorological station (the list of instruments is given in the text); the area indicated by the dotted circle corresponds to wetter and higher vegetation (see text).

(1993). They have a 15 cm aperture and operate at a wavelength of 0.94 μm, with a square signal modulated at 7 kHz to discriminate between light emitted by the transmitter and that of ambient radiation. The data were sampled every second and averaged over 15 min time steps. The instruments deliver an output voltage

V (volts) and $C_N{}^2$ is computed as $C_N{}^2 = 10^{(V-12)}$. The standard deviation of V (σ_V) was also recorded. So as to avoid possible interference between instruments, their paths were separated by 10 m, and the transmitter and receiver alternated (Fig. 1b). Prior to the experiment they had been installed at the same height (3.45 m) on different masts over 1 day for inter-calibration purposes (DOY 231–232). Then they were deployed at three heights (2.50, 3.45 and 6.45 m) to perform $C_T{}^2$-profile measurements between DOY 249 and 254 (6–11 September). The path length crosses the humid area previously mentioned over a distance about 80 m long approximately occupying its second quarter (between ∼70 and ∼150 m) from its SW extremity (see Fig. 1b). As (i) this area spreads towards the east of the path length to a few tens of metres upwind and as (ii) it is situated in the vicinity of the middle of the path where the sensitivity of scintillometers is maximum, it is likely to have an influence on the measurements.

A 3D Applied Technology [3] sonic anemometer (height: 4.0 m, sampling frequency: 10 Hz, orientation towards SE in the prevailing wind direction) was installed in the center of the experimental set-up (referred to as 'central site' in what follows) to provide reference measurements of sensible heat flux. It was also used to estimate the roughness length. During the experiment we observed a large range of unstable conditions with $-z/L$ values varying from 0.002 up to 10. The quality of the eddy correlation measurements was assessed by comparing our instrument against two other 3D Solent R3 Gill [4] sonic anemometers, one in Mexico during the experiment, the other in France a few weeks after the end of the experiment: we found an excellent agreement $H_{AT} = 1.017 H_{R3}$ ($r^2 = 0.982$) for 776 samples (30 min integration time) and fluxes ranging up to 250 W m^{-2}. On a neighbouring micrometeorological mast, measurements of wind speed at 2.68 m and wind direction (using a Campbell [5] cup anemometer and wind vane), net radiation at 2.50 m (REBS Q6 instrument [6]), air temperature and humidity at 3.0 m (Vaisala HMP 35 [7]) were performed. Two soil heat flux plates had also been installed in the vicinity of the surface at ∼5 mm depth (one under vegetation, the other under a bare soil patch). The heat storage in the soil layer above the soil heat flux plates was neglected. As the vegetation is quite similar at the central site and in the fetch upwind, with possible small scale non-homogeneities only, we consider the local reference measurements (3D and micrometeorological) satisfactorily allow to characterise the drier part of the landscape. But no reliable information on fluxes above the wetter area was available.

3.2. Inter-comparison of the scintillometers

The inter-comparison experiment was performed over a 24 h period, between DOY 231 (8:00 a.m.) and DOY 232 (9:00 a.m.). The three scintillometers were placed at the same height (3.45 m), and were sampling parallel optical paths 10 m apart. As we have no independent estimation of $C_N{}^2$, the mean value of the three measurements ($C_{N\,mean}{}^2$) was used as the reference. The general agreement between instruments is good (Fig. 2). Differences between measurements come from the combination of two sources of error:

- The first error — referred to as the calibration error — lies in systematic differences between instruments : two of the three instruments (A and C) differ by only 0.5%, while the third one (B) provides values smaller by about 2%. As perfect agreement between instruments A and B had been found in a previous calibration experiment (performed at Audenge, in the south-west of France over a fallow field in 1997 and for a larger range of $C_N{}^2$ values), such a difference is difficult to understand: is it a drift of the instrument itself or is it simply related to possible variations in surface conditions along the different parallel optical paths?
- The second error — referred to as the instrumental error — depends on the scintillometers' accuracy and corresponds to the scatter around the regression lines established for each instrument. Its evaluation requires a more important data set both displaying large variation in $C_N{}^2$ values and including enough runs for significant statistical study. We

[3] The name of the companies are given for the benefit of the reader and do not imply any endorsement of the product or company by the authors.
[4] Same as Footnote 3.
[5] Same as Footnote 3.
[6] Same as Footnote 3.
[7] Same as Footnote 3.

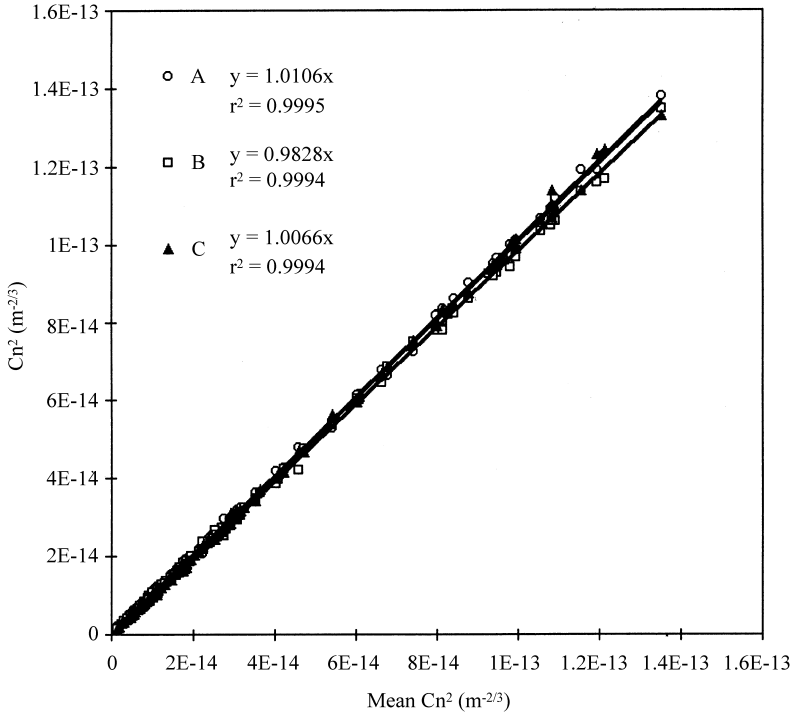

Fig. 2. Inter-calibration of the three scintillometers. The *x*-axis represents the average value of the three measured C_N^2. The 'forced through 0' regressions are also indicated.

therefore based the characterisation of the instrumental error on instruments A and B only for which more inter-calibration data were available: 408 runs, 10 min integration time each, C_N^2 up to $7 \times 10^{-13}\,m^{-2/3}$, by merging Zapata (Mexico 1998) and Audenge (France 1997) inter-comparison experiments. Analysis of the data showed that, at least over the range of the observed C_N^2, the absolute error (defined as the absolute value of the deviation of every measurement from the regression line between the two instruments, $|\Delta C_N^2|$) was increasing with C_N^2. We therefore analysed the measurement uncertainties in terms of relative error $|\Delta C_N^2|/C_N^2$. To avoid artefacts due to possible artificial increase of the relative error for small C_N^2 values, we eliminated the points corresponding to $C_N^2 < 2 \times 10^{-14}$ which generally correspond to night time conditions. The histogram of the relative instrumental error indicates that it follows a normal distribution with a 5% standard deviation (Fig. 3).

A longer inter-calibration experiment would have been necessary to evaluate the accuracy of the three scintillometers together with more confidence. For future experiments we strongly recommend an inter-comparison over several days, sampling a wide range of C_N^2 values (by performing measurements in drier conditions and/or by placing the instruments at a lower height).

3.3. Estimation of roughness length and displacement height

The roughness length z_0 was estimated from wind speed (u), friction velocity (u_*) and Monin–Obukhov length (L) values all measured directly by the 3D instrument, using Eq. (6). In this case we used $z = z_{3D} - d$, z_{3D} and d being the height of the sonic anemometer and the displacement height, respectively.

As the vegetation height varies from 30 to 60 cm within the field, with a rather important cover fraction (at least 70%), we arbitrarily set d at 30 cm. The histogram of the realistic z_0 values retrieved in moderately unstable conditions, $-1 < z/L < 0$ (Fig. 4) shows we can reasonably take $z_0 = 10$ cm.

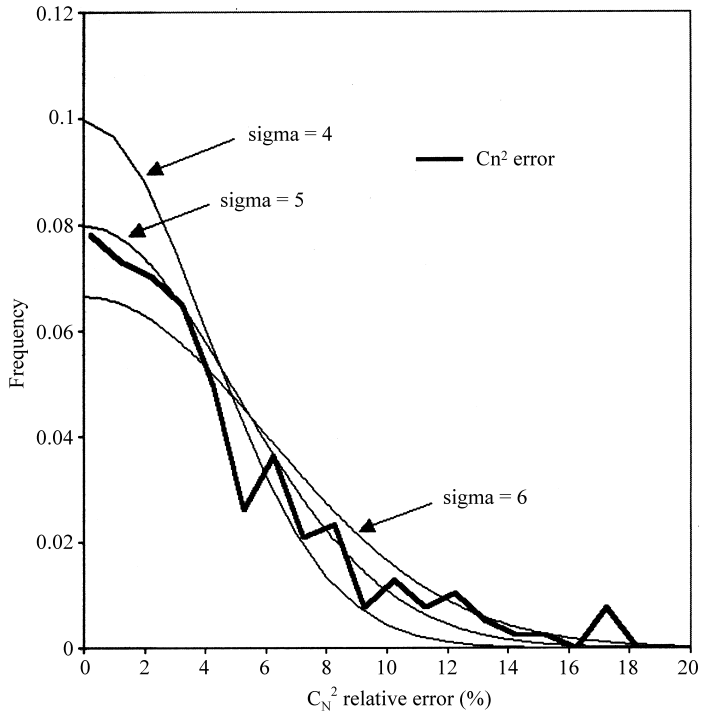

Fig. 3. Distribution of the relative measurement error on C_N^2 observed during the inter-calibration experiments performed in Audenge (south-west France, 1997) and in Zapata (Mexico, 1998). The normal distributions with standard deviations 4, 5 and 6.0% are also plotted.

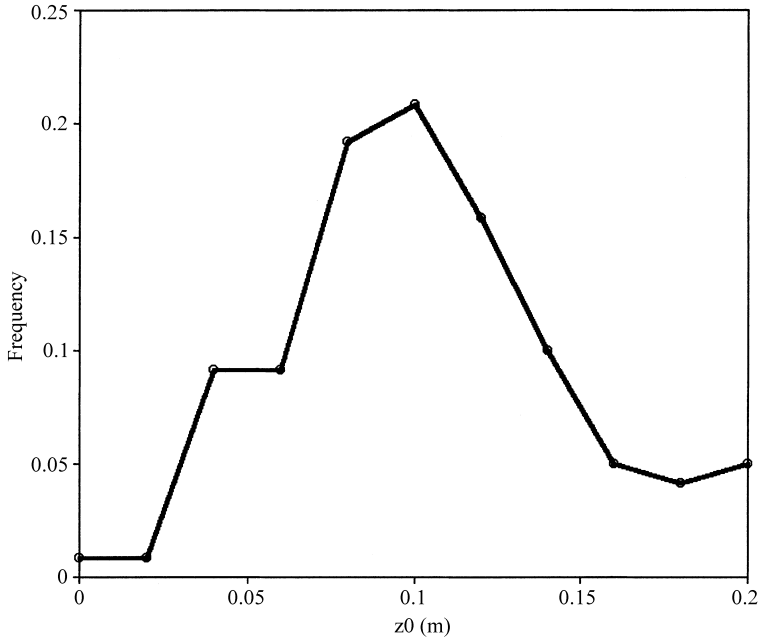

Fig. 4. Histogram of the roughness length values z_0 retrieved from 3D sonic anemometer measurements.

4. Experimental results

4.1. 1L method

In testing the C_T^2-profile method, we must first evaluate the consistency of the independent scintillometer measurements obtained at each level. We therefore present as a first step the estimations of sensible heat flux obtained by the 1L method.

Computations of u_* have been made using the wind speed measured at 2.68 m with the cup anemometer. Net radiation R_n and soil heat flux G from the central meteorological station provide the available energy $A = R_n - G$. G is the average of the measurements of the two soil heat flux plates. Accuracy on G is not a critical point for our purpose as G only indirectly appears in a corrective factor through the Bowen ratio β ($\beta = H/(A - H)$) in Eq. (1). Nevertheless, as the use of soil heat flux plates is subject to important well known uncertainties (due to the differences of thermal characteristics of soil and plates and to the difficulty of correcting for the thin soil layer above the plates, among others), we used the direct measurements of G only after having checked that they gave realistic estimates: the mean ratio G/R_n was found to be 0.21 for R_n values greater than 400 W m^{-2}, which is consistent with general experience.

Values obtained for each scintillometer are plotted against the eddy correlation measurements in Fig. 5. All the data have been used in a first step and no selection has been made on wind direction (most of the time perpendicular to the propagation path) or on the variability of C_N^2 during a run (Hill et al. (1992) eliminate 'nonstationary' runs for which the structure parameter varies by more than a factor 8). The three instruments provide similar estimates, but rather important scatter is visible and it appears that scintillometer measurements underestimate by about 15% the reference H_{3D}.

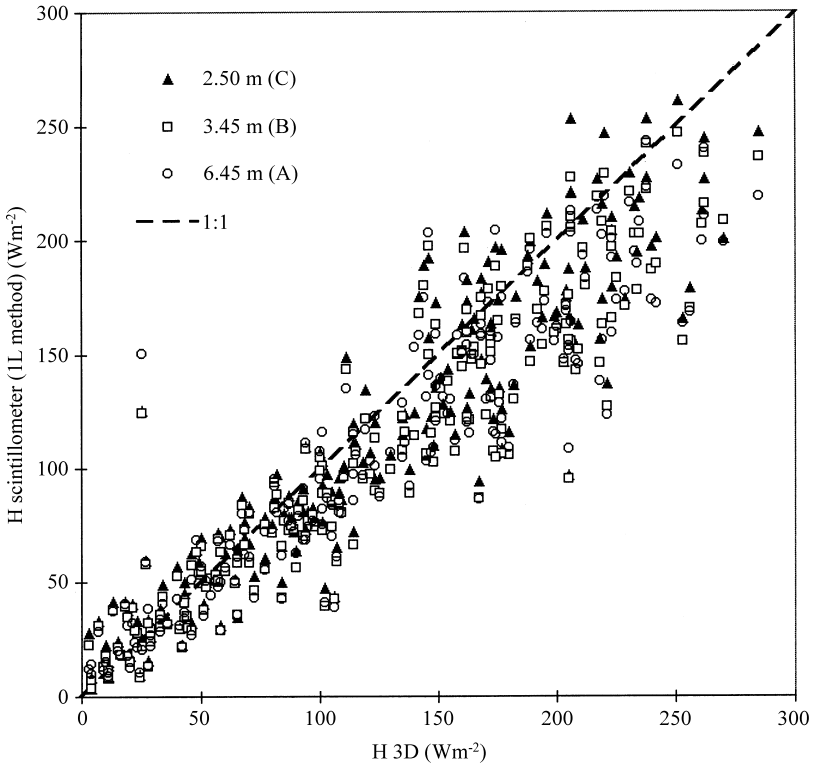

Fig. 5. Comparison of sensible heat flux estimated at Zapata site from the three scintillometers using the 1L method at every height independently against H measured using a 3D sonic anemometer.

The regression line obtained for the three instruments considered together is $H_{\text{scint}} = 0.862 H_{3D}$ with $r^2 = 0.870$ and an RMS error (RMSE) of 22.6 W m^{-2}. The slopes of the regression lines obtained for the three instruments considered separately are 0.841 (A), 0.849 (B) and 0.895 (C). Results of validation experiments of LASs performed by other authors (see for instance McAneney et al., 1995; De Bruin et al., 1995) are much better. A very severe filtering of 'nonstationary' runs by eliminating runs for which $\sigma_V > 150$ mV (which corresponds to a rejection of 40% of the data) did not bring significant improvement, but only a slight reduction of scatter. Similarly, the fact of selecting the most favourable wind direction conditions (from east to south, facing the 3D anemometer within a $\pm 45^\circ$ angle and crossing the scintillometer path at angles between 45 and 90°) is of no effect on the quality of the relation between scintillometer and 3D estimated fluxes. The non-homogeneity of the field is therefore likely to explain the observed deviation from the 1:1 line: as previously mentioned, the eddy correlation measurements were performed on a relatively drier area displaying a lower and sparser vegetation representative of the site, while the path of scintillometers were including an important proportion of a wetter area. No reliable reason could be found for explaining the large scatter.

So as to evaluate the $C_T{}^2$-profile method, it is important to check that there is no vertical divergence of sensible heat flux, and that the three scintillometers provide the same value whatever the height of measurement. Fig. 6 shows the estimates of H performed by every scintillometer against the mean value of the three measurements, $\langle H_{1L} \rangle$. This figure gives idea of the consistency of the scintillometers' response. The characteristics of the linear regressions $H_{\text{scint}} = \alpha \langle H_{1L} \rangle$ obtained are given in Table 1. Despite small systematic differences between the instruments, the

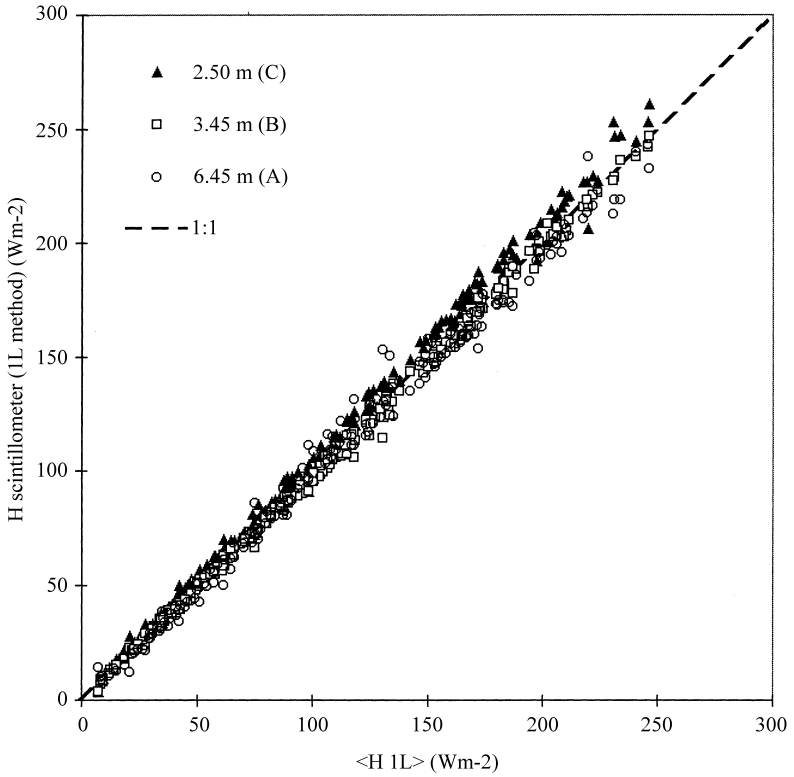

Fig. 6. Comparison of sensible heat flux estimated at Zapata site from the three scintillometers using the 1L method at every height independently against the mean H value $\langle H_{1L} \rangle$.

Table 1
Comparison of the sensible heat flux estimated using the 1L method at three different heights against the mean value of the three measurements $\langle H_{1L} \rangle$: the characteristics of the linear regressions $H_{scint} = \alpha \langle H_{1L} \rangle$ (223 runs available) are given

Levels and instrument	2.50 m (C)	3.45 m (B)	6.45 m (A)
Without inter-calibration			
α	1.037	0.985	0.979
RMSE ($W m^{-2}$)	4.0	2.7	5.4
With inter-calibration			
α	1.032	0.998	0.970
RMSE ($W m^{-2}$)	4.0	2.7	5.5

agreement is quite satisfactory. Merging the whole data set, we can consider that the three LAS provide a ±5% accuracy on the sensible heat flux. This control demonstrates: (i) the reliability of the three scintillometers' measurements and (ii) the fact that — as the retrieved sensible heat flux remains constant with height — the instruments are all placed in the surface boundary layer. The data set therefore appears consistent and quite suitable for testing the profile method which should provide similar fluxes in these conditions.

4.2. Profile method

The profile method has been applied in the three possible combinations of two levels (2.50 and 3.45 m), (2.50 and 6.45 m) and (3.45 and 6.45 m). No correction for inter-calibrating the instruments has been done in a first step. Because of the doubts about the representativity of the 3D sonic anemometer/eddy correlation measurements, we only present here the comparison against $\langle H_{1L} \rangle$ (Fig. 7). In addition to a deviation from the 1:1 line, it shows a considerable increase of the scatter whatever the couple of heights considered: Table 2 shows that the RMSE of the

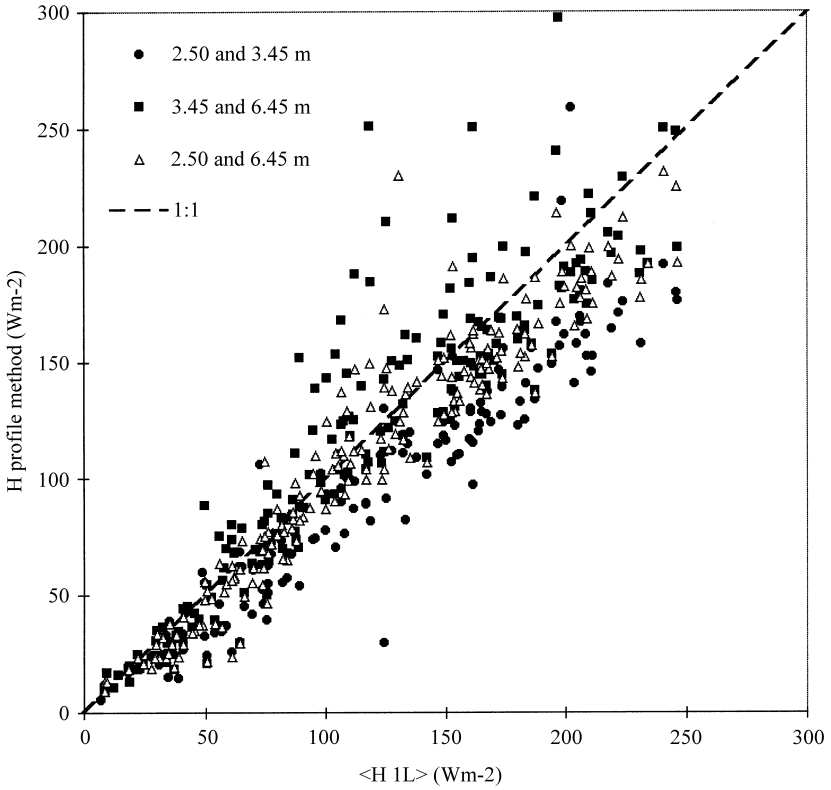

Fig. 7. Comparison of the sensible heat flux estimated at Zapata site by the C_T^2-profile method against $\langle H_{1L} \rangle$ for the three possible combinations of heights.

Table 2
Experimental results: characteristics of the comparisons between the sensible heat flux obtained using the $C_T{}^2$-profile method with different combinations of heights against the mean flux estimated using the 1L method $\langle H_{1L} \rangle$ (223 runs available)

Levels	2.50 and 3.45 m	3.45 and 6.45 m	2.50 and 6.45 m
Without inter-calibration			
α	0.788	0.994	0.920
r^2	0.892	0.843	0.909
RMSE	17.1	25.1	17.0
Rejection cases (%)	38.7	12.2	15.3
With inter-calibration			
α	0.875	0.934	0.905
r^2	0.881	0.839	0.911
RMSE	20.3	23.3	16.7
Rejection cases (%)	27.9	19.8	17.1

linear regressions $H_{\text{profile}} = \alpha \langle H_{1L} \rangle$ reaches $25\,\text{W}\,\text{m}^{-2}$ and is much larger than for the single level measurements. Moreover, critical problems appear in some cases (the occurrence of rejections is also indicated in Table 2): computations either may lead to unrealistic values not even plotted in Fig. 7 (out of scale), or they may simply be impossible, the estimated ratio r (Eq. (9)) being out of the range $1 < r < (z_2/z_1)^{2/3}$ previously defined (see Eq. (10)) for unstable conditions.

The failure of the profile method is easy to explain. For near-neutral conditions, $f(z/L)$ tends towards 4.9 (see Eqs. (3) and (4)) and the ratio r tends towards 1; the denominator of Eq. (10) then tends towards 0, making the computation of L subject to very large errors. These propagate on u_* through Eq. (5), which may lead to unrealistic values of $u_* T_*$. Similarly, under very unstable conditions, $r \to (z_2/z_1)^{2/3}$ and $L \to 0$ according to Eq. (10). $f(z/L)$ then tends towards 0 (see Eq. (3)), which possibly induces large errors on the estimate of T_* (see Eq. (2)) and finally on H.

As it determines that of r, the accuracy of $C_N{}^2$ measurements is therefore likely to limit the accuracy of estimates of H under atmospheric conditions (near neutral and highly unstable) in which H is over-sensitive to r. Computations may even be simply impossible when measurement errors on the structure parameters $C_{N1}{}^2$ and $C_{N2}{}^2$ at both heights or a poor inter-calibration of the instruments make the inequalities $r > 1$ (near neutrality) or $r < (z_2/z_1)^{2/3}$ (very unstable) to be not satisfied.

This is consistent with the results of other authors who have commented on the sensitivity of the profile method to the inter-calibration and accuracy of the scintillometers. Andreas (1988) already noted the uncertainties of the $C_T{}^2$-profile method for near-neutral conditions and under highly unstable conditions. Hill et al. (1992) compared scintillometer derived sensible heat flux H and friction velocity u_* using the $C_T{}^2$-profile method against eddy correlation measurements on a small data set: they attributed to systematic differences between their scintillometers the rather poor agreement they observed for H and the systematic deviation for u_*.

Following recommendations given by Hill et al. (1992), we also tested the results obtained with inter-calibrated data (1L and profile methods). For this, we used 'inter-calibrated' $C_N{}^2$ values retrieved from the regressions indicated in Fig. 2. The results are presented in Tables 1 and 2. No significant improvement appears when comparing with the previous results obtained with raw (i.e. non-calibrated) $C_N{}^2$ values.

At this point of the study one may conclude from the experimental results that:

1. Provided z_0 is known, the 1L method is much more robust than the profile method. The profile method is very sensitive to measurement errors, particularly in near neutral and very unstable conditions.
2. The possible improvement brought by a careful inter-calibration of the scintillometers before using the profile method, as recommended by several authors, could not be fully addressed with our data set. The reasons lie in the poor confidence we have in our inter-calibration experiment. First the experiment was too short (only 1 day). Secondly it suffered from the lack of a credible independent reference measurement of $C_N{}^2$. This probably translates into a remaining bias (underestimation as depicted in Table 2), when comparing the profile method retrieved fluxes after calibration against $\langle H_{1L} \rangle$ ($\langle H_{1L} \rangle$ being quasi-insensitive to calibration corrections, see Table 1).
3. The choice of the measurement heights may be crucial: Table 2 shows that the worst results (in terms of rejection cases and deviation of slope α from the 1:1 line) are obtained when scintillometers are near the ground and close to each other.

4. Additionally, because of prevailing humid conditions (due to repeated rainfall events during the 1998 summer), our experimental data set did not cover the whole range of possible sensible heat flux values and atmospheric stability conditions.

So as to generalise from these preliminary conclusions and to define the limits of the profile method more precisely, we performed a simple modelling experiment described below.

5. Simulation

5.1. Principle

The first step computes the exact values of $C_N{}^2$ at three different heights from a prescribed value of sensible heat flux for a given surface and micrometeorological conditions. Then, realistic noise is added to the $C_N{}^2$ values. The third step involves computing H using the profile method. These steps are detailed below. Finally, the derived H values are compared to the prescribed ones. For comparison purposes, we also repeated the same procedure with the 1L method.

For a surface characterised by its roughness length and displacement height (prescribed values), simulation runs were performed over a large range of H and of atmospheric stability conditions (though we only focus on unstable conditions in this paper). The data required were wind speed at a given reference height, air temperature and net radiation. Practically a run is performed as follows:

1. u_* is first calculated using an iterative procedure combining Eq. (6) and an expression of Monin–Obukhov length. L is corrected for humidity following Panofsky and Dutton (1984) as

$$L = -\frac{\rho c_p T_a {u_*}^3}{kgH(1 + 0.07/\beta)} \tag{12}$$

The Bowen ratio is estimated as $\beta = H/(R_n - H - G)$) where the ground heat flux G is here taken as $G = 0.15R_n$. T_* is then computed as $T_* = H/\rho c_p u_*$. $C_T{}^2$ can then be estimated from Eqs. (2) and (3). Finally $C_N{}^2$ is computed using Eq. (1).

2. Realistic errors (in terms of magnitude and statistical distribution) are then assigned to $C_N{}^2$.
   - In what follows we first examine the sensitivity to instrumental errors only. For this purpose the exact $C_{Ni}{}^2$ values at level i ($i = 1, 2$ or 3 for the three scintillometers) are replaced by $C_{Ni}{}^2$ $(1 + 0.01\delta_i)$. The relative errors δ_i (expressed in percent) for each instrument are randomly selected for every run from three normal distributions having the same prescribed standard deviation (σ). The three errors are therefore independent from each other.
   - A second step evaluates the sensitivity to calibration errors only. The instrumental errors are now set to 0, and every $C_{Ni}{}^2$ ($i = 1, 2, 3$) value is modified by a systematic error, i.e. replaced by $(1+\varepsilon_i)C_{Ni}{}^2$, ε_i depending on the instrument (i.e. the measurement height) only, and being kept constant for all the runs.
3. H is finally computed again applying the profile method as described in Section 2.3.

All the simulations have been made with a constant net radiation of 550 W m^{-2} and air temperature of 30°C. Reference height is 4 m. In order to have a range of z/L values as large as possible, the sensible heat flux H and wind speed u are given random values (with a uniform distribution) and allowed to vary between 0 and 450 W m^{-2} and between 0.5 and 6.0 m s^{-1}, respectively. For each simulation 4000 runs are repeated. Before performing the sensitivity study, we first checked the code by assigning a 0 value to $C_N{}^2$ errors and verifying the H flux initially prescribed was correctly retrieved.

5.2. Sensitivity to instrumental errors

5.2.1. Simulation of Zapata data

We used the scintillometer heights (i.e. 2.50, 3.45 and 6.45 m) and surface characteristics (i.e. $z_0 = 10$ cm and $d = 30$ cm) encountered on the Zapata site. We assumed that the instruments were perfectly inter-calibrated and that measurements were only affected by instrumental errors δ_i ($i = 1, 2, 3$). Four simulations have been performed assuming standard deviations (σ) of instrumental errors of 2.0, 3.0, 4.0 and 5.0% successively, the latter corresponding to the order of magnitude found after the inter-comparison experiment (see Section 3.2).

Table 3 shows the statistics for the regression between simulated — by both 1L and profile methods

Table 3
Effect of the instrumental error on scintillometer measurements on the sensible heat flux (H) accuracy for the 1L and profile methods. The distribution of the relative error on C_N^2 is assumed to be normal and four standard deviation cases are tested ($\sigma = 2, 3, 4,$ and 5%). The correlation coefficient (r^2) and the RMSE of the linear regressions $H_{\text{simulated}} = \alpha H_{\text{prescribed}}$ are given both for 1L and C_T^2-profile methods. The percentage of rejected computations is also indicated

	1L method			Profile method		
Height (m)	2.50	3.45	6.45	2.50 and 3.45	3.45 and 6.45	2.50 and 6.45
$\sigma = 2$						
α	1.000	0.9996	0.9993	1.023	1.012	1.008
r^2	0.9994	0.9994	0.9993	0.8939	0.9824	0.9912
RMSE	2.96	3.12	3.34	42.20	16.67	11.77
Rejection cases (%)	0	0	0	8.5	4.0	1.7
$\sigma = 3$						
α	0.999	1.000	0.999	1.031	1.023	1.016
r^2	0.9984	0.9983	0.9982	0.8301	0.9449	0.9691
RMSE	5.01	5.16	5.38	55.58	30.06	22.27
Rejection cases (%)	0	0	0	15.2	6.6	3.0
$\sigma = 4$						
α	1.000	1.000	0.999	1.020	1.030	1.021
r^2	0.9971	0.9971	0.9967	0.8035	0.9137	0.9477
RMSE	6.82	6.78	7.29	60.66	38.52	29.27
Rejection cases (%)	0	0	0	21.6	9.9	5.1
$\sigma = 5$						
α	1.000	1.000	1.000	1.020	1.038	1.026
r^2	0.9954	0.9953	0.9949	0.7632	0.8860	0.9279
RMSE	8.61	8.69	9.03	68.04	44.86	34.41
Rejection cases (%)	0	0	0	28.0	12.6	7.0

— and prescribed H values, $H_{\text{simulated}} = \alpha H_{\text{prescribed}}$, forced through the origin. Table 3 also gives the percentage of rejection cases (impossible computations or unrealistic results). Fig. 8a and b illustrates results for $\sigma = 5\%$. The scatter remains very large whatever the combination of heights considered: the RMSE characterises the standard deviation of the error on simulated H values and varies between 34 W m^{-2} (for 2.50 and 6.45 m combined heights) and 68 W m^{-2} (for 2.50 and 3.45 m). To give an idea, if we assume the error in H follows a normal distribution, an RMSE of 30 W m^{-2} (which means that 99% of the points are within a $\pm$90 W m^{-2} interval) roughly corresponds to a $\pm$30% relative accuracy on H (whose average prescribed value is around 300 W m^{-2}).

For comparison, Fig. 8c shows that the sensitivity of the classical 1L method to instrumental errors is much more limited, the simulated H not differing from its prescribed value by more than $\pm$6%. Table 3 shows that, whatever the instrumental error σ, the accuracy of the 1L method is at least four times better than the profile method. It also appears that the accuracy of the profile method is reduced significantly when the two heights of measurement are close to each other and/or close to the ground. The simulations confirm that the instrumental errors can be responsible for the impossibility of performing retrievals in a number of cases (up to 28%, see Table 3). These impossibilities are encountered near neutrality, or for high atmospheric unstability, for which computations must be rejected. This may limit the usefulness of the profile method for practical applications, for instance when a continuous monitoring of sensible heat flux is expected.

After having confirmed by these simulations the sensitivity to instrumental errors, as observed in our experimental results (see Section 4.2), the question now rises if a suitable choice of the measurement heights would yield a better performance from the C_T^2-profile method.

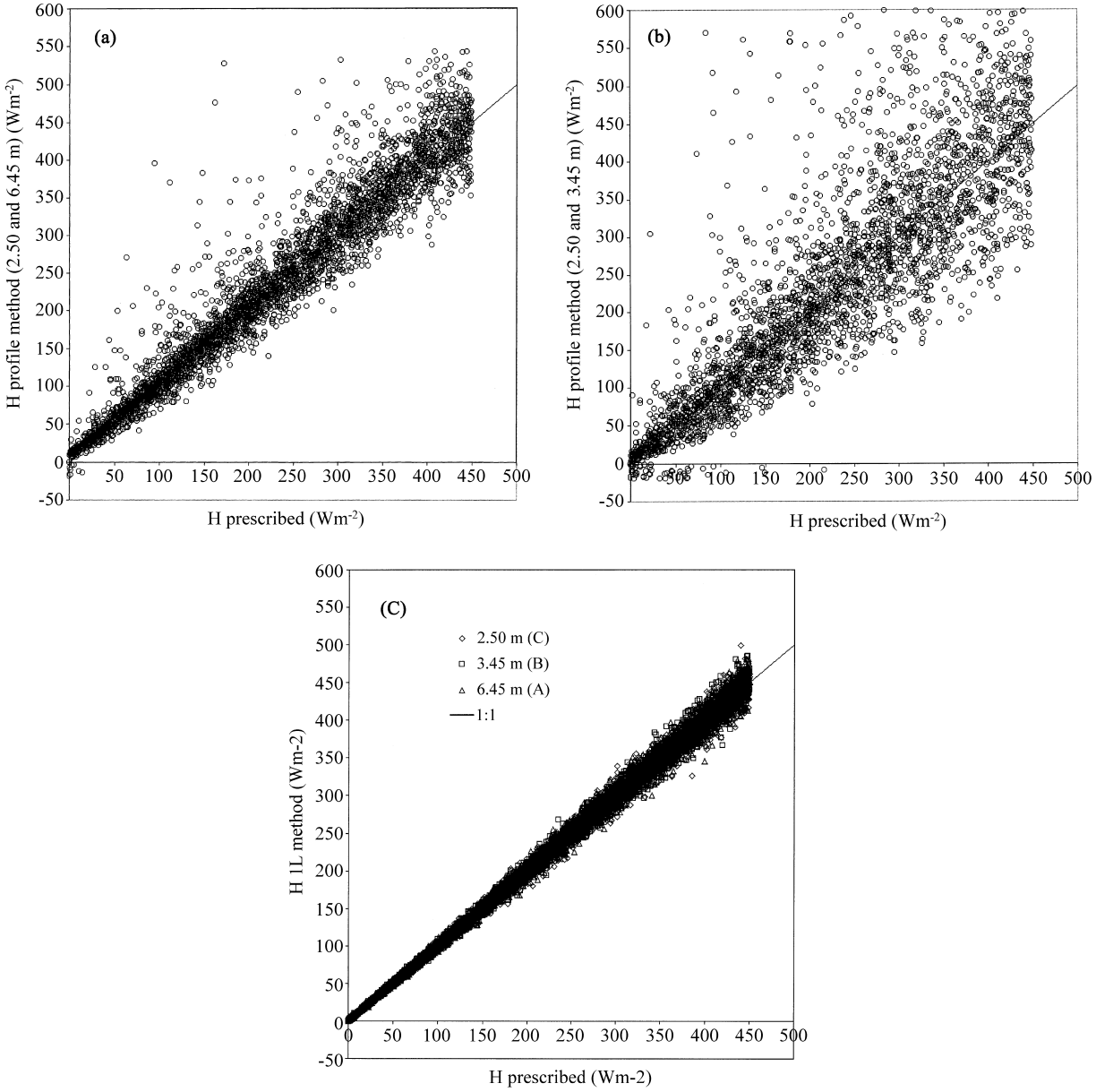

Fig. 8. Simulation of the sensible heat flux using the C_T^2-profile method, assuming a relative instrumental error following a normal distribution with a 5.0% standard deviation, and for different combinations of scintillometer heights (a: 2.50 and 6.45 m; b: 2.50 and 3.45 m). For comparison purposes, the simulation using the 1L method for each scintillometer is given in Fig. 8c.

5.2.2. Effect of height of the instruments

Andreas (1988) showed that the larger the ratio of measurement heights, the more accurate the determination of z/L by the profile method. He also discussed the practical constraints imposed by the location of the instruments, not too close to the surface for the lower one, and inside the surface boundary layer for the upper one.

We performed simulations to test the sensitivity of the profile method to the heights of instruments. All

Table 4
Combinations of heights (indicated by symbol x) used to test the sensitivity of the C_T^2-profile method to the location of scintillometers

z_1 (m)	z_2 (m)					
	3.45	5.0	6.45	7.5	10	15
2.5	x	x	x	x	x	x
3.45			x			
5.0					x	x
7.5						x

the configurations tested are indicated in Table 4. They allowed us to test the sensitivity of z_2/z_1 ratios ranging between 1.38 and 6. The lower level z_1 must be chosen with a particular care. As a matter of fact, in the framework of similar previous experiments over grass (not yet published), the comparison between sensible heat fluxes estimated by the classical 1L method at two heights revealed systematic underestimation of H for too small z_1 (lower than 2 m). Hill et al. (1992) mention the same problem with a scintillometer placed at 1.45 m. Moreover, for long propagation paths, LAS measurements are more prone to saturation if performed close to the ground. The saturation distance depends on the characteristics of LAS: for instance, according to Hartogensis (1997) who used the same instrument as ours, H fluxes up to 500 W m^{-2} can be measured only on distances under 500 m at 1 m height and under 700 m at 2 m height. For these reasons, we performed our simulations with $z_1 \geqslant 2.5$ m. The other constraint imposed by the surface boundary layer height for the choice of z_2 also contributes to limit the ratio z_2/z_1 for practical applications.

As the C_T^2-profile shape — and consequently the C_T^2 ratio at two given heights — obviously depends on the aerodynamic characteristics of the surface, we tested two cases: (i) $z_0 = 10$ cm and $d = 30$ cm (as in the Zapata site) and (ii) $z_0 = 2$ cm and $d = 0$ cm (which typically corresponds to short grass). Finally computations were done for three values of the standard deviation of the instrumental error, $\sigma = 2$, 3 and 5%. We only present here synthetic results illustrating the impact on two variables: the RMSE for H and the percentage of rejection cases.

Fig. 9a shows the variation of the RMSE on H against the z_2/z_1 ratio, the lower height z_1 being kept constant ($z_1 = 2.5$ m). The RMSE first rapidly

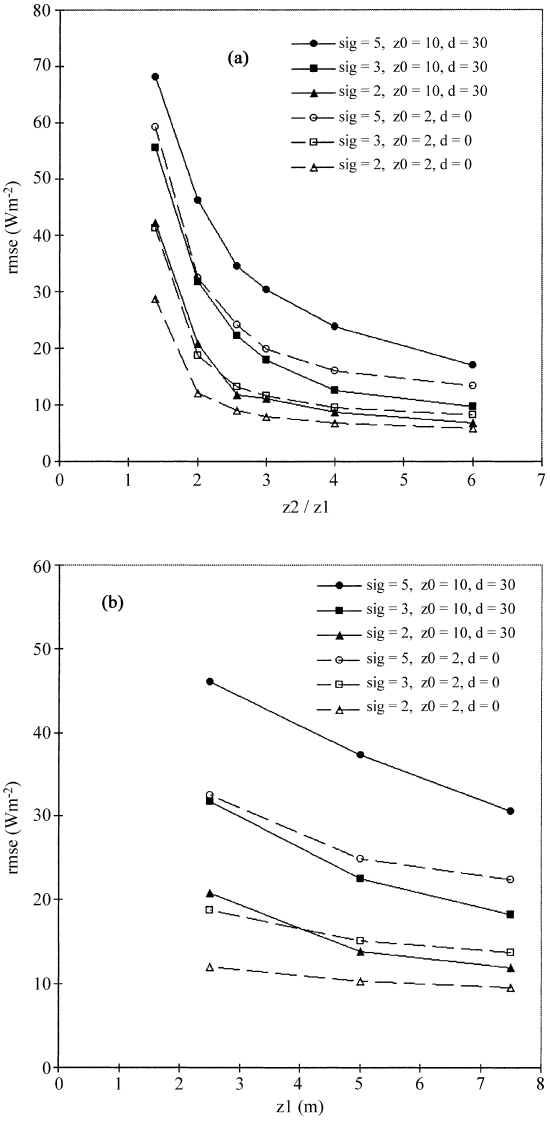

Fig. 9. Simulation study of the sensitivity of the C_T^2-profile method to the respective locations of the scintillometers. (a) RMS retrieval error for H vs. the ratio z_2/z_1 (using the same lower height $z_1 = 2.5$ m); (b) RMS retrieval error for H as a function of the lower height z_1 (for a given height ratio $z_2/z_1 = 2$). Three cases of instrumental errors have been tested ($\sigma = 2\%$: triangles, $\sigma = 3\%$: squares and $\sigma = 5\%$: circles), as well as two surface types ('high' vegetation: full lines, and 'low' vegetation: dotted lines).

decreases with z_2/z_1 and it remains rather constant for z_2/z_1 ratios greater than 4. The RMSE is obviously larger for important instrumental noise, whatever the aerodynamic characteristics of the surface, as it can

easily be seen in Fig. 9a. High values of z_2/z_1 (∼6) tend to reduce the sensitivity of the instrumental error on H, but are not easily compatible with the practical constraints discussed above. We also note that for a given combination of heights, the $C_T{}^2$-profile method is more robust above low vegetation cover. For a given height ratio ($z_2/z_1 = 2$, Fig. 9b) one can see the best accuracy on H is obtained for the highest possible levels. The percentage of rejection cases rapidly decreases with z_2/z_1 for $z_1 = 2.5$ m (Fig. 10a). But for the given ratio $z_2/z_1 = 2$, it behaves differently from the RMSE and increases with z_1 (Fig. 10b). For a given location of instruments, the percentage of rejection is very sensitive to the instrumental error and to the roughness of the surface.

Simulations finally show that the best trade off is achieved by choosing $z_2/z_1 \sim 3$ or 4 with $z_1 \sim 2$ or 2.5 m. It is compatible with the practical constraints encountered for locating the instruments, i.e.: (i) the highest level remains below the top of the surface boundary-layer and (ii) the lowest level is above a minimum height from the surface so as to avoid underestimated measurements of $C_N{}^2$. In these conditions, the greatest accuracy attainable for H would be about ±10% (RMSE ∼10 W m^{-2}) obtained with a hypothetical instrument having a precision characterised by a $\sigma = 2\%$ normal distribution of the relative error. This is to be compared to an accuracy for H of about ±30% (RMS ∼25 W m^{-2}) obtained with a more realistic instrument having a lower relative accuracy ($\sigma = 5\%$). For the same ratio of heights, Fig. 10a shows that the percentage of rejection cases varies between 2 and 12% depending on the type of surface and the accuracy of scintillometers (instrumental error). A rapid degradation of these performances occurs when the height of scintillometers is altered.

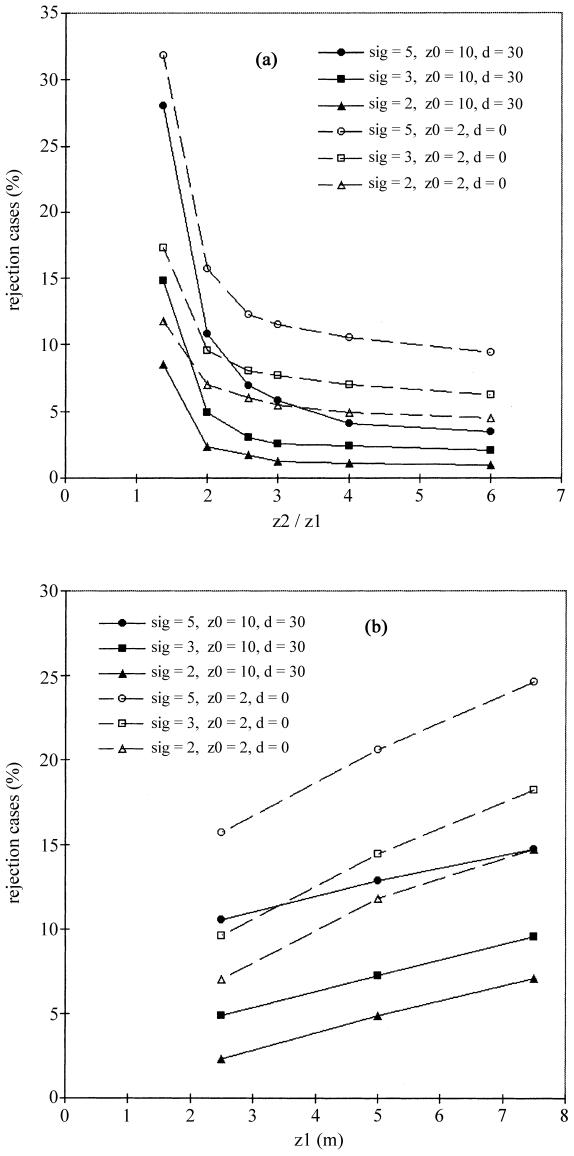

Fig. 10. Same as Fig. 9, but for the percentage of rejection cases ($C_T{}^2$-profile method leading to impossible computations or unrealistic results).

5.3. Sensitivity to calibration errors

The instrumental error has been here set to 0, and only a calibration error has been simulated. For this purpose, systematic deviations ε_i ($i = 1, 2, 3$) from the exact $C_N{}^2$ value were introduced on each instrument response. We did not performed a systematic study of the effect of instruments' miscalibration, but limited us to a few examples based on the case studies depicted in Table 5 to illustrate the possible errors for H. The sensitivity tests have been made using measurement heights of 2.5, 5.0, and 10.0 m, with $z_0 = 10$ cm and $d = 30$ cm for the characteristics of the surface. We only considered the combinations of levels including the lowest height $z_1 = 2.5$ m, i.e. (2.5 and 5.0 m) and (2.5 and 10.0 m). For clarity, we only present here cases for which instruments deviate symmetri-

Table 5
Sets of calibration errors (in %) introduced for testing the C_T^2-profile method. For each of the four cases, the sensitivity study has been performed for the combination of levels (z_1, z_2) and (z_1, z_3)

Case	Deviation (%)			
	1	2	3	4
ε_3 ($z_3 = 10.0$ m)	−1	+1	−2	+2
ε_2 ($z_2 = 5.0$ m)	−1	+1	−2	+2
ε_1 ($z_1 = 2.5$ m)	+1	−1	+2	−2

cally from the 1:1 line with opposite signs. But we controlled that the results were quite similar if only one of the instruments was affected by an equivalent overall error: for instance cases (−2%, +2%) and (0%, +4%) or (−4%, 0%) provided the same results. At least for small calibration errors, which seems to be important is the difference of calibration of both instruments. We evaluated the consequences of differences in calibration of up to ±4% (cases 3 and 4) between instruments.

Fig. 11 displays the comparison between simulated and prescribed H values obtained when combining the two lower levels (2.5 and 5.0 m) and simulating a +4 and −4% calibration difference successively between instruments. The two cases 3 and 4 (see Table 5) are gathered in Fig. 11: combined calibration errors of −2 and +2% for the lower and upper instrument, respectively induce a systematic overestimation of H (see circles); on the opposite, triangles in the same figure correspond to a simulation performed with calibrations errors of +2 and −2% (at lower and upper levels of measurement, respectively). Despite this being a worst scenario (even though Nieveen and

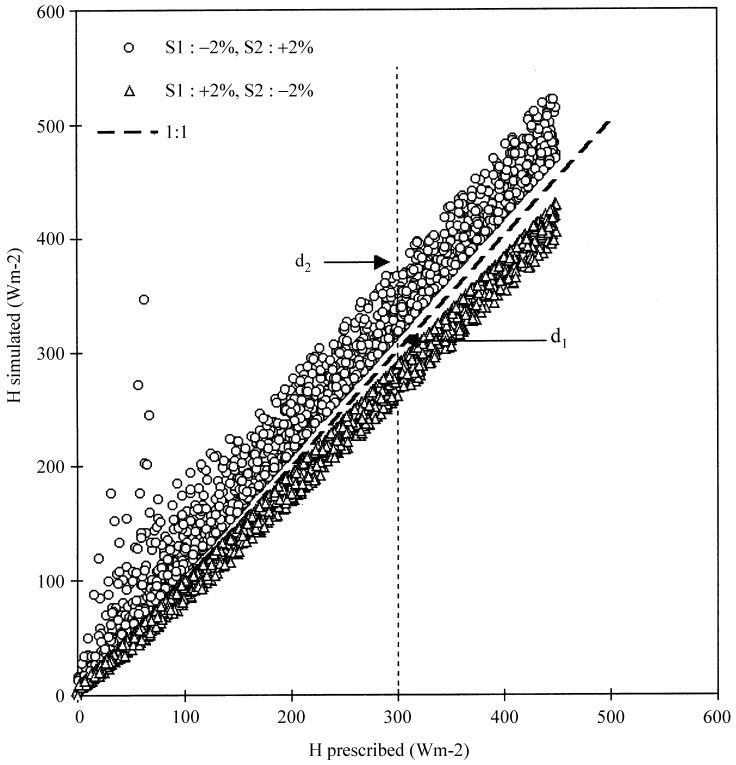

Fig. 11. Simulation study of the sensitivity of the C_T^2-profile method to inter-calibration errors. The example given here has been done for scintillometers located at 2.50 and 3.45 m; two cases of 4% inter-calibration difference between instruments have been tested: circles correspond to combined calibration errors of −2 and +2% for the lower and upper instruments, respectively; similarly triangles correspond to a (+2%, −2%) set of calibration errors. The deviations d_1 and d_2 from the 1:1 line at an arbitrary value $H = 300\,\mathrm{W\,m^{-2}}$ allow to characterise the scatter (see text).

Green (1999) found a 5% deviation on one of their instruments), it is given to introduce the criteria used in next figure: the scatter for H and its systematic deviation from the 1:1 line can simply be characterised by considering the two relative deviations d_1 and d_2 from the 1:1 line at an arbitrary H value (we took $H \sim 300\,\mathrm{W\,m^{-2}}$, see Fig. 11). d_1 and d_2 provide a helpful, despite qualitative, criteria to evaluate different configurations of calibration errors in what follows.

A synthesis of the results is presented in Fig. 12. The calibration difference between the two considered instruments ('high' minus 'low') is plotted along the x-axis. The y-axis represents the relative error on the retrieved H values (for $H \sim 300\,\mathrm{W\,m^{-2}}$) which ranges between the extreme values d_1 and d_2 previously defined. d_1 and d_2 increase (in absolute value) with the difference of calibration between the instruments. This defines an area (grey tones in Fig. 12) containing the possible values of the error for H. As an example, we see in Fig. 12 that for two instruments placed at 2.5 and 5 m and having a 3% difference in calibration, the error is likely to situate between −3 and −9% or between +3 and +15% depending on the fact either the upper or lower instrument is over-calibrated. Fig. 12 shows three such 'error areas' corresponding to the $C_T{}^2$-profile method applied to heights of: (i) 2.5 and 5.0 m, (ii) 2.5 and 10.0 m, and (iii) to the classical 1L method (given here for comparison purposes).

It appears that the lowest levels (2.5 and 5.0 m) tend to cause the largest errors on H. The sensitivity of the profile method to measurement errors when both instruments are placed too near from the surface is confirmed, as it had already been pointed out for the instrumental error (see Section 5.2). When the calibration of both instruments is satisfactory (say

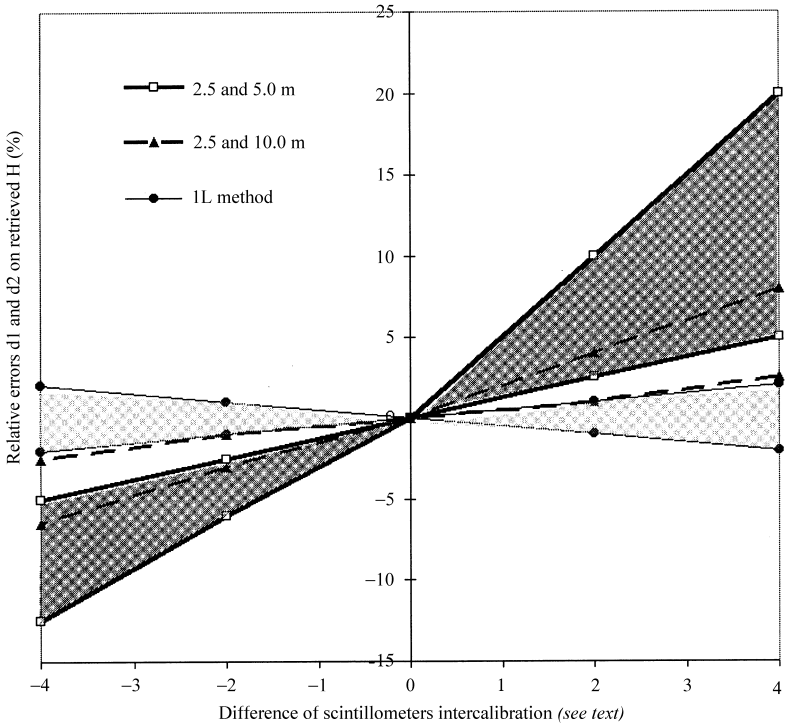

Fig. 12. Sensitivity of the $C_T{}^2$-profile method to inter-calibration errors: for a given combination of heights the relative errors on H resulting from inter-calibration differences between the two instruments (x-axis) are situated in an area between two curves. The thick lines and the dark grey area correspond to a combination of scintillometers' heights of 2.5 and 5.0 m, respectively; the dotted lines correspond to the combination of heights 2.5 and 10.0 m. For comparison purpose, the thin lines indicate the sensitivity of the 1L method to inter-calibration errors (clear grey area).

within ±1%), the resulting error on H is much smaller than the one induced by instrumental error. This confirms the small influence we noted on our experimental results when introducing a calibration correction. Choosing a larger z_2/z_1 ratio (levels 2.5 and 10 m) reduces the sensitivity to calibration error to a few percent, as indicated by the dotted lines in Fig. 12. The 1L method is the most robust, the resulting error on H being of the same order of magnitude as the calibration error with no amplification effect (see thin continuous lines in Fig. 12).

6. Discussion

An experiment combining measurements of scintillations with LASs placed at three heights (2.50, 3.45 and 6.45 m) over natural grassland (330 m propagation path) in Mexico was designed to test the potential of C_T^2-profile method for estimating sensible heat flux H. The classical method (1L) which consists in measuring scintillations at a single level but which requires an independent estimation of u_* has also been used for comparison purposes. The results confirm the robustness of the 1L method, provided the roughness length is correctly estimated. The comparison between the C_T^2-profile method derived H against the average of the 1L method estimations (taken as a reference) shows considerable scatter, particularly when the two levels used are close to each other and/or close to the surface. The RMSE is about 5 W m^{-2} for the 1L method, compared with the 17–25 W m^{-2} RMSE range obtained with the profile method (depending on the combinations of levels used). The experiment reveals significant limitations of the profile method: namely unrealistic estimations of H and the impossibility of performing the computations in either near-neutral conditions or very unstable conditions. These limitations are easily explained by the sensitivity of the equations used to measurement errors through the ratio between C_T^2 at two heights. Numerical simulations confirm these results.

Two types of measurement error on C_N^2 are identified. The 'calibration error' corresponds to a systematic deviation of the scintillometer response from the actual values of C_N^2. What we refer to as the 'instrumental error' corresponds to the scatter around a calibration curve. We assumed this to be random noise (Gaussian distribution). The inter-calibration experiment performed did not allow us to characterise precisely these two errors. For future experiments, we recommend a careful inter-calibration procedure.

The numerical experiments consisted of simulating actual C_N^2 data by adding a noise to exact C_N^2 values computed from prescribed H over a given surface, and then retrieving H by both the classical 1L and C_T^2-profile methods. Comparison between computed and prescribed H values allowed an evaluation of both methods. For instrumental error (expressed in terms of relative error) we tested the effect of Gaussian distributions of noise with standard deviation ranging between 2 and 5%. For the calibration error we examined the effect of differences between instruments up to ±4%.

The simulations confirmed the experimental results: the sensitivity of the C_T^2-profile method to measurement errors is likely to explain the large scatter we observed on Mexico data set. The sensitivity to instrumental errors appears so large in many cases that, even with a good inter-calibration of the scintillometers, the C_T^2-profile method remains prone to large errors. The simulations showed that the closer to the ground or to each other are the instruments, the higher is the sensitivity to instrumental errors. It also shows that the profile method is much more sensitive to measurement errors than the 1L method. For both calibration and instrumental errors, the simulations indicated that the larger the difference between measurement heights is, the better the estimations of H are. This condition is not always easy to fulfil: the upper level must be in the surface boundary layer, while the lower one must not be too close to the surface. A combination of measurement heights around 2.5 and 10 m generally provides a good trade off for vegetation heights of 50 cm or less. The characteristics of the surface also play a role, and we have shown that results were better for a vegetation with low roughness and displacement height.

Let us insist on the fact that, in this paper, we only tested the sensitivity of the 1L and C_T^2-profile methods to C_N^2 measurement errors. The profile method is 'self-sufficient' to estimate H whilst the 1L method requires to know the roughness length, which introduces another source of error, not taken into account in this paper. A rule of thumb estimation of z_0 is realistic for a dense homogeneous vegetation and allows a robust estimation of H (McAneney et al., 1995). This might not be the case for heterogeneous

vegetation or composite surfaces for which the definition of an 'equivalent roughness' still remains unclear and poses problems of aggregation; the consequence of z_0 errors on the final accuracy for H should be evaluated in these cases. Despite this, the over-sensitivity of the profile method to C_N^2 errors is likely to make it less competitive than the 1L method for estimating H.

Another limitation of the C_T^2-profile method lies in a number of cases for which computations are impossible or results unrealistic. They occur for near-neutral or very unstable conditions. The number of 'rejection' cases depends on the location of instruments and on the aerodynamic characteristics of the surface, but may reach as much as 30% according to the experimental results and to the simulations. This may drastically limit the practical interest of the profile method when a continuous monitoring of fluxes is desired.

Acknowledgements

The authors are indebted to CNES/TOAB (Centre National d'Etudes Spatiales/Terre Ocean Atmosphere Biosphere) and IRD (Institut de Recherche en Développement) who funded this study, and to the IRD/IMADES (Instituto del Medio Ambiente y el Desarrollo Sustentable del Estado de Sonora) who supported the field experiment.

Part of this study has been carried out in the context of a joint research project on scintillometry with the Department of Meteorology of the Wageningen University, who also provided the instruments.

References

Andreas, E.L., 1988. Atmospheric stability from scintillation measurements. Appl. Opt. 27 (11), 2241–2246.

Avissar, R., 1991. A statistical-dynamical approach to parameterize subgrid-scale land-surface heterogeneity in climate models. Surv. Geophys. 12, 155–178.

Brunet, Y., 1996. La représentation des paysages et la modélisation dans le domaine de l'environnement. In: Tendances Nouvelles en Modélisation, Pour L'Environnement. Elsevier, Paris, pp. 59–77.

Chehbouni, A., Njoku, E.G., Lhomme, J.P., Kerr, Y.H., 1995. Approaches for averaging surface parameters and fluxes over heterogeneous terrain. J. Climate 8, 1386–1393.

De Bruin, H.A.R., Van den Hurk, B.J.J.M., Kohsiek, W., 1995. The scintillation method tested over a dry vineyard area. Boundary-Layer Meteorol. 76, 25–40.

Goodrich, D.C., et al., 1998. An overview of the 1998 activities of the semi-arid Land-Surface Program. In: Proceedings of the 1998 American Meteorological Society meeting, Phoenix, AZ, pp. 1–7.

Green, A.E., McAneney, K.J., Astill, M.S., 1994. Surface layer scintillation measurements of daytime heat and momentum fluxes. Boundary-Layer Meteorol. 68, 357–373.

Green, A.E., McAneney, K.J., Lagouarde, J.P., 1997. Sensible heat and momentum flux measurement with an optical inner scale meter. Agric. For. Meteorol. 85, 259–267.

Hartogensis, O., 1997. Measuring areally-averaged sensible heat fluxes with a Large Aperture Scintillometer. Report. Department of Meteorology, Agricultural University of Wageningen, Netherlands.

Hill, R.J., 1992. Review of optical scintillation methods of measuring the refractive-index spectrum, inner scale and surface fluxes. Waves Random Media 2, 179–201.

Hill, R.J., Ochs, G.R., Wilson, J.J., 1992. Surface-layer fluxes measured using the C_T^2-profile method. J. Atmos. Ocean. Technol. 9 (5), 526–537.

Kaimal, J.C., Finnigan, J.J., 1994. Atmospheric Boundary Layer Flows: Their Structure and Measurement. Oxford University Press, Oxford.

Lagouarde, J.P., McAneney, K.J., Green, A.E., 1996. Spatially-averaged measurements of sensible heat flux using scintillations: first results above a heterogeneous surface. In: Proceedings of the Workshop on Scaling-up in Hydrology Using Remote Sensing Workshop, June 10–12, 1996, Institute of Hydrology, Wallingford, UK. Wiley, New York, pp. 147–160.

McAneney, K.J., Green, A.E., Astill, M.S., 1995. Large-aperture scintillometry: the homogeneous case. Agric. For. Meteorol. 76, 149–162.

Nieveen, J.P., Green, A.E., 1999. Measuring sensible heat flux over pasture using the C_T^2-profile method. Boundary-Layer Meteorol. 91, 23–35.

Noilhan, J., Lacarrère, P., 1995. GCM grid-scale evaporation from mesoscale modelling. J. Climate 8, 206–223.

Ochs, G.R., Cartwright, W.D., 1980. Optical system model IV for space-averaged wind and C_N^2 measurements. NOAA Technical Memorandum ERL WPL-52. NOAA Environmental Research Laboratories, Boulder, CO.

Ochs, G.R., Wilson, J.J., 1993. A second-generation large-aperture scintillometer. NOAA Technical Memorandum ERL WPL-232. NOAA Environmental Research Laboratories, Boulder, CO.

Panofsky, H.A., Dutton, J.A., 1984. Atmospheric Turbulence: Models and Methods for Engineering Applications. Wiley, New York.

Raupach, M.R., 1995. Vegetation–atmosphere interaction and surface conductance at leaf, canopy and regional scales. Agric. For. Meteorol. 73, 151–179.

Raupach, M.R., Finnigan, J.J., 1995. Scale issues in boundary-layer meteorology: surface energy balance in heterogeneous terrain. Hydrol. Processes 9, 589–612.

Wyngaard, J.C., 1973. On surface-layer turbulence. In: Proceedings of the Workshop on Micrometeorology. American Meteorological Society, Denver, CO, pp. 101–149.